

Article

A Dual Monitoring Technique to Detect Power Quality Transients Based on the Fourth-Order Spectrogram

Juan-José González-de-la-Rosa ^{*,†} , Agustín Agüera-Pérez [†] , José-Carlos Palomares-Salas [†] ,
Olivia Florencias-Oliveros [†]  and José-María Sierra-Fernández [†] 

Research Group Plan Andaluz Investigación Desarrollo Tecnológico e Innovación-Tecnologías de la Información y Comunicación-168 (PAIDI-TIC-168): Computational Instrumentation and Industrial Electronics (ICEI), Area of Electronics, University of Cádiz, Higher Polytechnic School, Av. Ramón Puyol S/N, E-11202 Algeciras, Spain; agustin.aguera@uca.es (A.A.-P.); josecarlos.palomares@uca.es (J.-C.P.-S.); olivia.florencias@uca.es (O.F.-O.); josemaria.sierra@uca.es (J.-M.S.-F.)

* Correspondence: juanjose.delarosa@uca.es; Tel.: +34-956-028-069

† These authors contributed equally to this work.

Received: 1 February 2018; Accepted: 22 February 2018; Published: 27 February 2018

Abstract: This paper presents a higher-order statistics-based approach of detecting transients that uses the fourth-order discrete spectrogram to monitor the power supply in a node of the domestic smart grid. Taking advantage of the mixed time–frequency domain information, the method allows for the transient detection and the subsequent identification of the potential area in which the fault takes place. The proposed method is evaluated through real power-line signals from the Spanish electrical grid. Thanks to the peakedness enhancement capability of the higher-order spectra, the results show that the procedure is able to detect low-level transients, which are likely ignored by the traditional detection procedures, where the concern pertains to power reliability (not oriented to micro grids), and this, by analyzing the duration and frequency content of the electrical perturbation, may indicate prospective faulty states of elements in a grid. Easy to implement in a hand-held instrument, the computational strategy has a 5 Hz resolution in the range 0–500 Hz and a 50 Hz resolution in the range of 0–5 kHz, and could be consequently used by technicians in order to allocate new types of transients originated by the distributed energy resources. Four real-life case-studies illustrate the performance.

Keywords: higher-order statistics; micro grids; power quality (PQ); spectral kurtosis (SK); spectrogram; time–frequency analysis; transient detection

1. Introduction

Nowadays the uncontrolled growth of the distributed energy resources (DERs) within the context of the smart grid (SG) has triggered new innovative solutions that take into account how consumers assess electricity service. The modern SG and the micro grids, with more power due to distributed generation (DG), requires sophisticated measurement methods not only for adequate power quality (PQ) surveillance but also for targeting the potential causes of the fault and assessing the importance of low-level events, such as solar photovoltaic (PV) energy, solar thermal energy, wind energy, fuel cells, energy storage, demand response (DR), and electric vehicles (EV). These newly perturbations, not characterized yet, have a direct impact on utilities and customers as well; e.g., an increase in nonlinear behavior of loads and equipment.

During the last three decades, instruments are incorporating new functionalities to perform such PQ measurements. For reasons based on the complexity of the electrical network and the considerable

increase of the measuring points, it should be added that there is no need to measure a specific type of disturbance among the classical within the norm EN50160 [1] and that the storage and data processing requirements depend very much on specific needs. Despite the fact that fixed instruments have been spread throughout the entire network thanks to last mile communication systems and that PQ features are being included in smart meters and automation equipment, there is no instrument that meets the needs of every customer. In an attempt to test customers' needs, it was reported in [2] that utilities and TSOs (transmission system operators) mainly use fixed PQ monitors, while DSOs (distributed system operators) handle portable analyzers. The selection of the measurement locations depends on the customers' needs and the sensitivity of the site under test. Indeed, the criteria used to select the instruments are mainly based on the equipment's performance regarding the specific problem, as opposed to the normative issues and technical support after purchase [2].

A current challenge in PQ monitoring systems is the detection of low-level perturbations and the isolation of a potentially faulty element that may affect the micro storage systems' performance. Indeed, one of the major concerns of instrumentation manufacturers is associated with online transient detection and discrimination, as it eventually may lead to an assessment of the cause–effect relationship. Consequently, the research in this branch constitutes a challenging task that involves utilities, researchers, and final users.

This article presents a contribution to the class of instruments considered as “transient detectors,” which is based on the fourth-order spectrogram. The fourth-order spectrum, a higher-order statistics (HOS) approach in the frequency domain, enhances the peakedness of the frequency components enabling the detection of transients. The time-sliding version, the fourth-order spectrogram, is postulated in the present work to measure the length of the transient along with the frequency content of the electrical disturbance. This double information may increase the probability of targeting the malfunctioning element in scenarios with a high degree of DERs.

Along with the higher-order time–frequency duality based on the spectral kurtosis (SK), the computational strategy is settled on two main pillars. The method presents two possible resolution operating modes, within two different frequency ranges, depending on the transient under test: a 5 Hz resolution in the range 0–500 Hz and a 50 Hz resolution in the range of 0–5 kHz, which is currently the focus of the new instrumentation design [3]. Secondly, the computational strategy, based on the SK, accounts for variability over a 100-register set: the new segment in the analysis window and 99 realizations of noise processes. If the test window comes across a transient that it is not present in the remaining 99 registers, the event is labeled with a probability of 100% in the spectrogram, a color is associated with the probability of the transient occurrence, and this situation does not change until the transient vanishes independently of its amplitude. The 100 noise signals constitute a database used to detect any kind of signal different from noise. According to former experiences in the research team, the SK analysis over 100 signals has enough sensitivity to detect coupled PQ disturbances [4].

To illustrate the measurement sequence, four real-life measurement registers have been selected and analyzed in this work. From the experimental set of results, a two-fold conclusion is set regarding this methodology. Thanks to the fast Fourier transform (FFT) method, the SK increases the detection speed substantially [5,6]. It also has a strong noise rejection capability conferred by the HOS [5], as the transient frequency is outlined over the noise floor, even for low-level transients. This method may be used as a fine frequency location and afterwards the power spectrum can be used to reformulate new power quality indexes.

The layout of the paper is as follows: The review of the transient nature of the electrical grid is exposed in Section 2. Section 3 summarizes the main outcomes regarding transients' measurements in power systems. Afterwards, the computational strategy is presented in Section 4, which deals with the advantages of HOS and their introduction into smart meters within the frame of load scheduling. Results are gathered in Section 5. Conclusions and prospective work are detailed in Section 6.

2. The Transient Scenario of the SG

The electrical grid is under the direct influence of a variety of transients that similarly affect the electrical grid from its historical origins to the current state of development. Along with the transients, the technology regarding protection devices has evolved with the aim of configuring a shield for the susceptible equipment. The mission of the protection devices consists of deviating the spurious transients to the ground.

There are myriads of transient sources, which range from lightning to different kinds of those produced by equipment (e.g., switches, capacitors banks, and equipment in the consumer's side). All of them are coupled to the grid's conductors via different mechanisms, according to their associated physical principles. Most transients have low energy content, but the magnitudes of some, such as lightning-induced transients, are sufficient to damage most electronic equipment.

Along with the mentioned sources of transients, as a consequence of the grid's development, the DERs are connected to the grid without proper planning and consequently have a deep impact on the quality of the energy; e.g., photovoltaic panels and medium-size wind turbines are connected using conductors with low losses, but with the handicap of the introduction of high frequency transients that spread through the grid. The shapes and duration of these transients are entirely new and unpredictable. In fact, switching the transients' characteristics depends on the system's electrical parameters, e.g., resistance, capacitance, and inductance. At the same time, the induced transients, being a DER under the effects of lightning, will also be induced in the SG. Consequently, the final user in a building is directly exposed to the lightning and switching phenomena [7].

In this frame, most of the electronic equipment is highly susceptible to electrical anomalies. Some industrial equipment subject to such anomalies include programmable logic controllers, uninterruptible power supplies, metering devices, heating, ventilation, and air conditioning systems, and communication units. Additionally, we find susceptible equipment, e.g., health-care units and urban measurement and control systems, beyond the industrial world. Finally, control electronic units of the distribution elements that control the flux of electrical power are also the targets of PQ events [3,7]. A perturbation in any of this equipment can cause fatal disasters.

Certain factors highly determine the susceptibility of equipment: the unpredictable origin of the transients, the coupling mechanism through which the transient penetrates in the equipment, and the impedance between the source and the equipment. On this basis, protection methods are continuously being deployed and basically pivot around intercepting and attenuating transients at the entrance point of the facility which supplies the electricity. This first modulating action is then complemented via additional protection devices, installed in the distribution panels and the final use location [3,8,9].

3. PQ Monitoring Systems and Transient Meters

Monitoring systems and data analysis from power systems have been in focus over the last twenty years, particularly the design of new architectures and newly added features that have arisen in the class of smart analyzers. Commercial versions are now capable of analyzing trends in power systems and are widely used in energy-efficiency-oriented industrial applications. Most versions have included innovative signal processing modules that extract the necessary features from the signal under test, with the goal of classifying the PQ disturbances, especially the transients [10].

To establish a reference, the branch of equipment for PQ analysis was treated in depth in [11]: architectures, installation, and issues regarding capturing tendencies of the monitoring systems were exposed. Wagner et al. [12,13] identified common disturbances in production environments. The first formal guidelines for implementing monitoring systems were presented by Rauch et al. in [14] and by Liu in [9]. The global evolution and tendencies according to installation, architecture, and software performance was discussed by Sawyer in [15]. With regard to specific issues, the pros of using an object-oriented philosophy were elucidated in [16].

Several industrial-oriented software-based applications for disturbance detection and analysis have been developed. Among them, we remark the design proposed by Shakarijan et al. [17].

A subsequent version (enhanced in terms of communication and triggering) was conceived in 2004 by the team conducted by Daponte and was called *the TransientMeter*, which consisted of a monitoring system oriented to detect and classify transient disturbances based on wavelets transforms. Its performance was acceptable under controlled conditions [10].

Regarding DSP solutions, three backgrounds have been selected. Bucci et al. [18] designed a distributed virtual instrument, based on LabVIEWTM, thought to monitor the steady-state electrical anomalies (mainly sags, swells, and flickers) and to measure precise parameters (amplitude, duration, and rise and fall times). Likewise, it is also worth mentioning the work by Chung-Ping et al. [19], who deployed a real-time control unit for multiple sources.

With respect to experiences in the public domain, it is well worth citing the research in [20], which examines PQ in public distribution electricity grids. Additionally, the work by Makinen et al. [21] is of high interest because it synthesizes the evolution of PQ monitoring systems in a country frame.

Having described the frame, the contribution of our work consists of an HOS-based approach to discriminate transients on an SG. The algorithm uses the fourth-order discrete spectrogram thought to monitor fault transients at nodes of the domestic grid. The combined time–frequency information enhances the transient detection and the subsequent identification of the potential faulty area. The proposed method is evaluated through real power-line signals from the Spanish domestic electrical grid. Thanks to the peakedness enhancement capability of the higher-order spectrum, it is shown that the method is able to detect low-amplitude transients that are likely ignored in traditional detection procedures (not oriented to micro grids), and this, by analyzing the duration and frequency content of the electrical perturbation, may indicate prospective faulty states of elements in a grid.

4. The Computational Strategy

4.1. Higher-Order Statistics and the Spectral Kurtosis

Estimates of higher-order cumulants are being used extensively in measurement systems to infer new statistical characteristics associated with data from a non-Gaussian time-series in a predominant Gaussian background floor, which can be theoretically considered as a result of the summation of different noise processes. Within the transient detection context, the target PQ event is always considered non-Gaussian, while the floor is assumed to be stationary Gaussian signal [4,22–24]. Thus, using HOS would help to locate the transient in a qualitative way, with a rough approximation.

Given an r th-order real-valued random process (measurement time-series), $x(t)$, the joint compacted notation for cumulants is expressed in Equation (1):

$$C_{r,x}(\tau_1, \tau_2, \dots, \tau_{r-1}) = \text{Cum}[x(t), x(t + \tau_1), x(t + \tau_2), \dots, x(t + \tau_{r-1})] \quad (1)$$

where τ_i is the i th time shift, which is a multiple of the data acquisition sampling period, T_s , usually expressed as $\tau_i = iT_s$. Normally, the statistical cumulants given by Equation (1) are estimated by using a compact formula (*Leonov-Shiryayev*), which expresses the compact relationship among the cumulants of stochastic time-series and their associated statistical moments [24].

HOS data in the frequency domain are arranged multi-dimensionally. Thus, these multi-dimensional structures or tensors (poly-spectra), the r th-order spectra, notated as $S_{r,x}(f_1, f_2, \dots, f_{r-1})$, are defined to be the $(r-1)$ -Fourier transforms of the r th-cumulants, in accordance with Equation (2):

$$S_{r,x} = \sum_{\tau_1=-\infty}^{\tau_1=+\infty} \cdots \sum_{\tau_{r-1}=-\infty}^{\tau_{r-1}=+\infty} C_{r,x} \cdot \exp[-j2\pi(f_1\tau_1 + f_2\tau_2 + \cdots + f_{r-1}\tau_{r-1})]. \quad (2)$$

Looking at computation issues, in general, poly-spectra consist of complex numbers, as can be inferred from Equation (2). For example, by making $r = 2, 3, 4$ in the former Equation (2), three traditional spectra are obtained: the power, bi- and tri-spectrum, respectively—the first one being real and the other two being complex magnitudes. For this reason, poly-spectra graphics contain a great deal of information, and their computation is unfeasible in the majority of the cases. Thus, one-dimensional slices and dual-frequency surfaces have to be extracted from the big-data tensors structures in order to obtain acute information regarding the phenomena under observation [24].

Regarding the statistical interpretation, while the bi-spectrum identifies the contributions to the statistical skewness as a function of frequency pairs, the so-called bi-frequencies, the tri-spectrum accounts for the contributions to the signal's kurtosis as a function of frequency triplets, or tri-frequencies [24].

A number of HOS estimators have been specifically designed to extract ad hoc information. Our focus is on the SK, which is a quantification of the statistical kurtosis associated with each Fourier component of a process (or time-series from a measurement instrument) and measures data time-series peakedness, which in turn allow for the identification of the transients. For estimation and notation issues, M measurement sweeps of the process are taken into account. Mathematically, each realization consists of an N -point vector; i.e., each time a measurement iteration takes place, and N points (spaced by the sampling period, T_s) are stored in one of the M vectors.

The novelty of the research consists of using the SK to target the frequencies with which the electrical perturbations are mostly associated. Then, a further FFT analysis may be developed in a subsequent stage to quantify the real effect of these frequencies on the system under test. The biased estimator for the SK for M sweeps of N points, and with a frequency index m , is given by Equation (3):

$$\hat{G}_{2,X}^{N,M}(m) = \frac{M}{M-1} \left[\frac{(M+1) \sum_{i=1}^M |X_i(m)|^4}{\left(\sum_{i=1}^M |X_i(m)|^2 \right)^2} - 2 \right] \quad (3)$$

where $X_i(m)$ is the m th Fourier component of the i th realization for the N -data vector x_i . This estimator sweeps the register (measurement time-series) under test. Its value ranges from zero to M for each frequency index, m [24]. Given a frequency index m , this maximum is the consequence of having the j -th sample, $|X_j(m)|$, notably higher than the rest, $|X_i(m)|$ with $i \neq j$. This fact is outlined in Equation (4) and denotes its capabilities for transient detection.

$$\hat{G}_{2,X,max}^{N,M}(m) \approx \frac{M}{M-1} \left[\frac{(M+1)|X_j(m)|^4}{(|X_j(m)|^2)^2} - 2 \right]. \quad (4)$$

The measurement range for the estimator will be considered in the experimental spectrograms.

4.2. The Computational Method and the Analysis Modules

The estimator described in Equation (3) is computed considering a number of $M = 100$ N -point realizations, according to the following strategy. Initially, for calibration issues, 100 white Gaussian noise processes are considered so that the SK value is null for all the frequencies. Then, one of these realizations is replaced by the first $N = 200$ data of the time-series under test. Using this strategy, we assure the full benefits of the SK, as it reveals the novelty in the following sense. If the added time-series is completely new in the set, the SK will take a different value and will rise abruptly.

The PQ data acquisition recommendations in IEEE 1159 refer to 512 samples/cycle (25.6 KHz) as the highest sampling frequency, typically used to monitor low-frequency signals, and these recommendations also refer to the voltage usually measured on a cycle-by-cycle basis [25]. Under these assumptions, the spectral analysis involves the following setup: a maximum frequency of 12.8 KHz,

a frequency resolution of 50 Hz, and a temporal resolution of 20 ms. Hereinafter, the data acquisition and processing based on these specifications will be named full surveillance analysis (FSA), and it will be used as a reference to determine the benefits of the proposed methodology. The FSA has two important drawbacks for an implementation in effective low-cost smart meters: firstly, the inability to certify the presence of inter-harmonics as they are separated exactly by 50 Hz, which coincides with the maximum frequency resolution (50 Hz). Thus, any other coupled signal would be indistinguishable from the nearest inter-harmonic. The second handicap is related to the sampling frequency, as it may not be reachable for most basic/low-cost devices. Consequently, this analysis includes the frequencies to survey oscillatory transients and higher harmonics, according to the standards IEC 61000-4-7 [26] and IEC 61000-4-30 [27].

The proposed two-stage strategy is thought to overcome former drawbacks. It detects low-frequency transients (<5 kHz, according to IEEE 1159 recommendations), keeps a temporal resolution of 20 ms, and, in this case, achieves a frequency resolution of 5 Hz below 500 Hz. This enables the detection of lower inter-harmonics and other events around the fundamental frequency. Additionally, the optimized specifications of the proposed strategy results in simpler electronic requirements for its implementation on smart meters: a lower sampling frequency, a lower number of processed data, and, consequently, lower memory requirements and less computational time.

This two-fold strategy is based on two computational modules. Thus, assuming a sampling frequency of $F_s = 10$ kHz, the low frequency module (LFM) works with a sub-sampled signal at $F_s = 1$ kHz, whereas the high frequency module (HFM) operates with the original record. Both the LFM and the HFM handle $M = 100$ realizations, each of $N = 200$ data. Thus, the FFT resolution is 5 Hz (500 Hz/100 data) within the 0–500 Hz range for the LFM, and 50 Hz (5000 Hz/100 data) in the 0–5000 Hz range for the HFM.

Regarding the number of cycles that are considered within the 200-point analysis window, the LFM accounts for 10 cycles (200 points $\cdot 10^{-3}$ s = 0.2 s), while the HFM only considers one cycle of the power-line signal (200 points $\cdot 10^{-4}$ s = 0.02 s).

Likewise, a complementary hybrid analysis provides high temporal resolution, which provides sensitivity to short events, a high frequency resolution in lower frequencies such that variations in the fundamental frequency and lower harmonics can be checked, and a top frequency of 5 kHz for higher harmonics. All of these features are implemented without a significant increase in computation time.

5. Experimental Results

Hereinafter, four case studies are analyzed in order to illustrate the proposed method. The experimental arrangement is shown in Figure 1. Data acquisition has been performed using a portable unit and a differential probe.

Figure 2 depicts the four types of disturbances to be detected. These have been directly measured at the Polytechnic School's building, running at a sampling frequency of 10 kHz. The tested faults include a specific (intermittent) harmonic distortion (Fault #1), an impulsive transient (Fault #2, *Dirac Delta*), an oscillatory transient (Fault #3), and a voltage sag of 0.15 s approximately (Fault #4). These four cases are representative of the faulty signals that may take place in this location. As a final remark before analyzing each case, it is worth mentioning that the four signals contain harmonics, which are considered to be constant disturbances in the building under study.

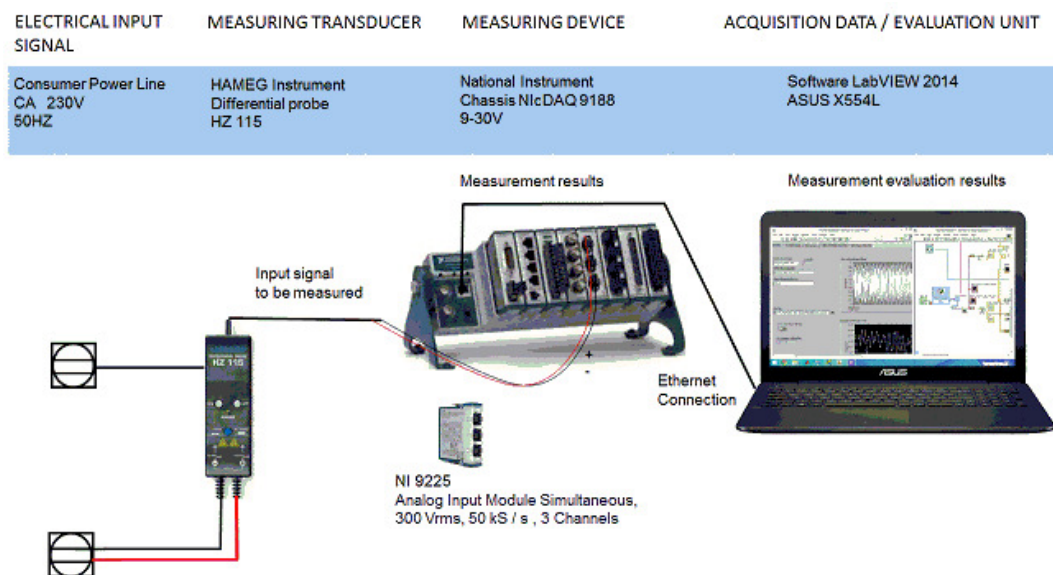


Figure 1. Experimental arrangement. A differential probe is connected to the power supply. The data are processed through labVIEW™.

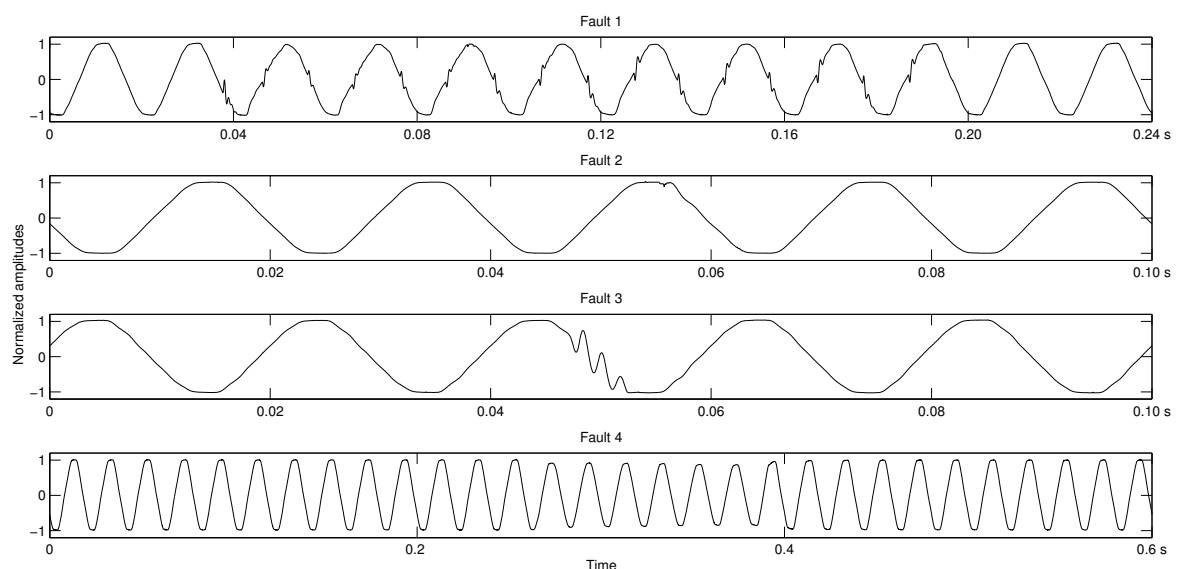


Figure 2. The four types of faulty signals under test. Fault #1: Harmonics. Fault #2: Impulsive transient (Dirac delta). Fault #3: Oscillatory transient (700 Hz). Fault #4: A voltage sag characterized by a duration of 0.15 s.

Figure 3 shows Fault #1, which illustrates that both significant deformation and long duration of the transients produce important deviations in the HFA and the LFA. The fault takes place within two 10-cycle segments of the LFM computation (between 0.4 and 0.8 s). The LFA shows the beginning of the event and the HFA reveals the harmonic/periodic structure in the 50–400 Hz (2nd, 4th, ..., harmonics). The 50 Hz resolution in the HFM cannot be used to determine the harmonic/periodic structure already commented (the result is a continuous red zone in low frequencies since harmonics are 50 Hz equally spaced, which is exactly the resolution of HFM). Additionally, inter-harmonics are targeted in the analysis, as indicated by IEEE 519-2014 [28] and IEEE 1159-2009 [25]. On the other hand, this analysis demarcates the limits of the event with a resolution of 1 cycle (between 0.56 s and 0.74 s) and reveals that the frequencies far from the fundamental component have a significant presence during the event.

Concretely, the frequencies around 900 Hz are associated with a kurtosis value of 100, revealing the periodic structure.

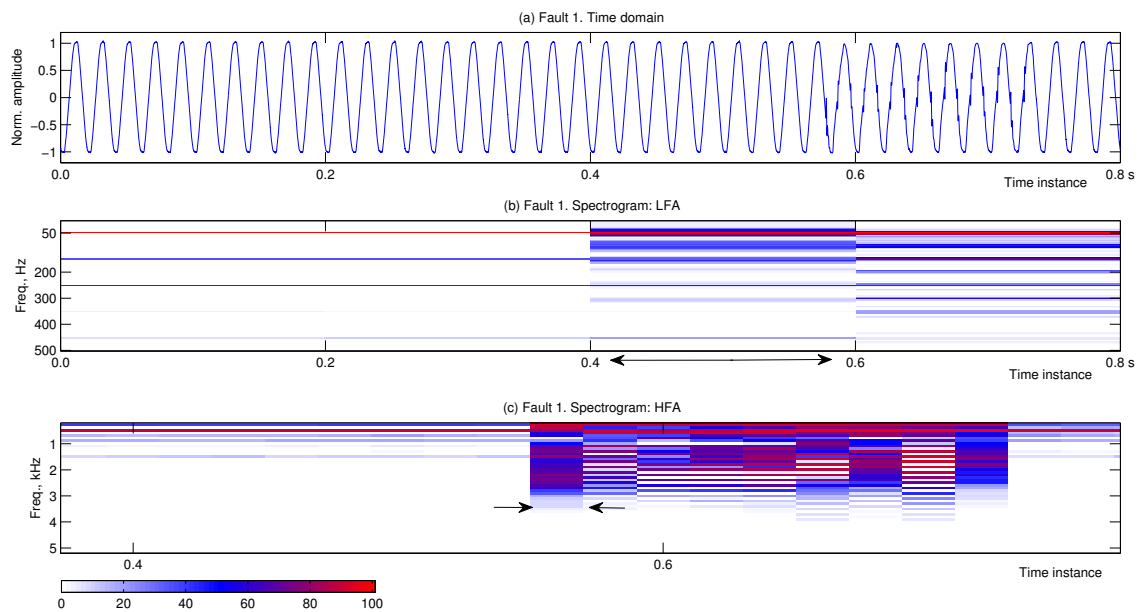


Figure 3. Fault #1: Harmonics. From top to bottom: the time domain signal, the LFA (a segment embraces 0.2 s), and the HFA (a segment is equivalent 0.02 s). The scale in the lower-left corner indicates the value of the PQ index. The arrows mark the segments limits.

Fault #2, whose analysis is shown in Figure 4, produces a minor deviation in the 50 Hz line, shown within the LFA; only the commented underlying harmonics are marked during the analyzed period. On the contrary, the event is targeted in the HFA for frequencies lower than 1 kHz.

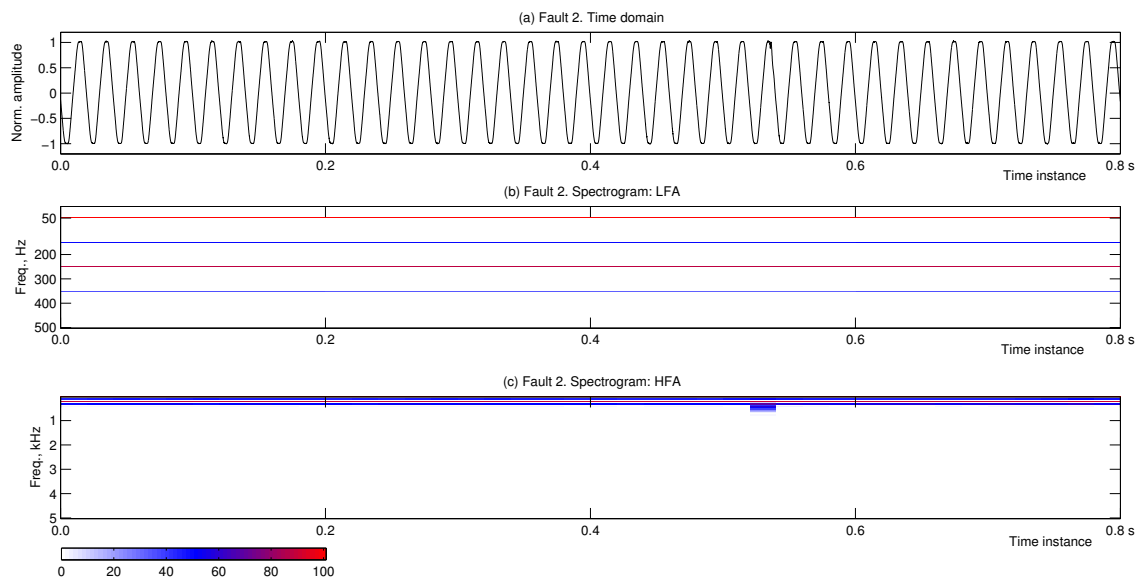


Figure 4. Fault #2: Impulsive transient (Dirac delta). Only the HFA, in the third subfigure, is capable of detecting the Dirac delta.

Fault #3 is depicted in Figure 5 and consists of a 700 Hz oscillatory transient with a duration of 8 ms. Focusing on LFA analysis, the event is short regarding the analyzed 10-cycle segment, but it

produces a soft footprint for frequencies higher than 250 Hz. In the HFA, the footprint is clearer and more accurately demarcated, revealing that the most relevant frequencies are centered around 700 Hz.

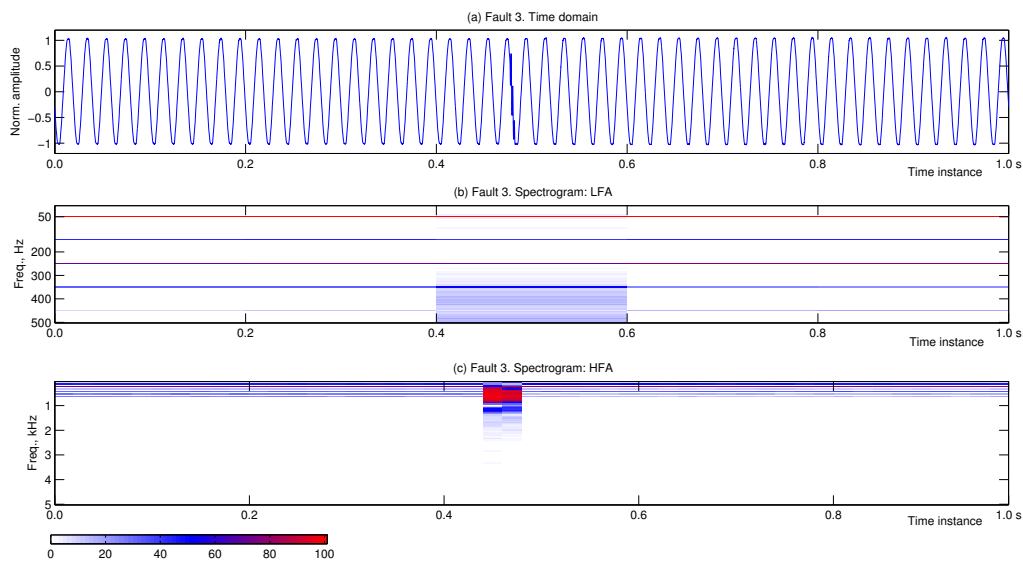


Figure 5. Fault #3: Oscillatory transient of 700 Hz and a duration of 8 ms (upper subfigure). The HFA module produces a more acute detection zone (third subfigure).

The fourth fault, depicted in Figure 6, is an 80% sag with a duration of 150 ms. It is entirely included in a 10-cycle segment of the LFM computation (the subgraph in the middle of Figure 6). In this analysis, the sag seems as it was a dispersion of frequencies around the underlying harmonics, as a result of the sudden change in the edge of the signal (change in the instantaneous frequency) (more intense in the 50 Hz). The HFM output demarcates the beginning and the end of the event, with variations in frequencies below the underlying harmonics. As opposed to the previously seen case studies, effects in the low zone of the frequency range are enclosed.

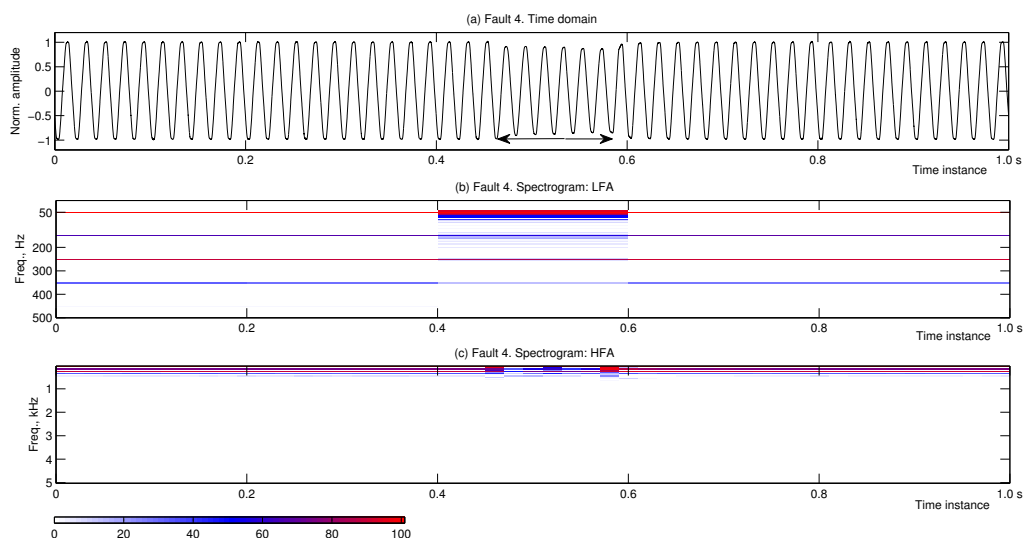


Figure 6. Fault #4: A sag with a remaining RMS voltage of 80%. The HFM output demarcates the beginning and the end of the event.

As has been demonstrated in former case studies, the simultaneous application of the two modules (LFM and HFM) offers highly detailed information in time (thanks to the 0.02 s resolution of

the HFM) and frequency domains, especially in the zone of the spectrum of major concern—around the fundamental frequency—thanks to the 5 Hz-resolution offered by the LFM module.

With the aim of quantifying the benefits of this approximation, we gather in Table 1 the experimental results associated with different strategies. The results are obtained using MATLAB™ (R2013a, The Math Works Inc., Natick, MA, USA), running under a processor Intel™ Core i5-2400, 3.1 GHz. (R2013a, The Math Works Inc., Natick, MA, USA). For a proper comparison of these computational strategies, an analysis reference base of 10 cycles of the power-line signal has been adopted. Results in Table 1 refer to this base. This is due to the fact that the hybrid analysis, whose advantages are to be shown, is completed every 10 cycles of the power-line signal. Indeed, for each of these cycles, an HFM analysis is developed, and, for Cycle 10, a double analysis (HFM and LFM) is performed; the LFA for the last cycle is developed via sub-sampling of the former 10 cycles (initially sampled at 10 kHz) at 1 kHz.

Table 1. Strategies for the measurement method (100 signals under test). The full option accounts for the total surveillance. The + sign indicates the options for the complementary HFM.

Magnitude\ Type of Analysis	FSA	LFA	HFA	Hybrid
Sample frEquation (F_s) (kHz)	25.6	1	10	10
Number of points within 10 cycles	5120	200	2000	2000 + 200
Number of analysis per 10 cycles	10	1	10	10 + 1
Top FrEquation (range) (kHz)	12.8	0.5	5	5
FrEquation resolution (Hz)	50	5	50	50 + 5
Temporal resolution (s)	0.02	0.2	0.02	0.02
Mean computation time per cycle (ms)	1.63	0.65	0.67	0.72

As shown in Table 1, the temporal resolution for the hybrid and the FSA analysis is the same, but the first one implies a lighter computational and hardware load: a computation time of 0.72 ms vs. 1.63 ms and a sampling frequency of 10 kHz vs. 25.6 kHz. The only disadvantage is related to the top frequency, but this frequency exceeds the analysis conditions (in Section 4.2).

In comparison with the individual performance of the LFM and HFM, the hybrid model takes the best parts of the two, as it supposes an average increment of approximately 7% of the computation time, in comparison with the individual application of each one.

Regarding the reliability of this computational approach, considering a database of 100 registers recorded from the domestic power supply, the method managed to detect 97% of the electrical disturbances. The two-fold concept (time–frequency) of the spectrogram made the identification more feasible and enabled a double-resolution analysis, features which cannot be addressed by static FFT computation.

6. Conclusions

This work has shown a frequency domain HOS approach to discriminate PQ events that commonly take place in the modern smart grid. The technique uses the fourth-order discrete spectrogram and benefits from mixed time–frequency domain information, which allows the potential area in which the fault takes place to be targeted. The computational strategy enables a 5 Hz resolution in the 0–500 Hz range and a 50 Hz resolution in the 0–5 kHz range to be reached.

The results show that the method detects low-amplitude transients that are likely ignored by traditional detection procedures (not oriented to micro grids), and this, by analyzing the duration and frequency content of the electrical perturbation, may indicate prospective faulty states of elements in a grid.

The computation options (the FSA, LFA, HFA, and hybrid methods) can be implemented in a hand-held instrument. The hybrid approach offers almost the same information as the full

surveillance mode but reduces the computation time; this feature postulates the hybrid module as an attractive option.

The proposed two-stage strategy detects low-frequency transients (<5 kHz), offers a temporal resolution of 20 ms, and achieves a frequency resolution of 5 Hz below 500 Hz (not achievable by a one-stage strategy for this temporal resolution). At the same time, the strategy results in simpler electronic specifications: a lower sampling frequency, a lower number of processed points, and, consequently, lower memory necessity and shorter computational time. Moreover, given that the computation time per cycle is 0.72 ms (Intel™ Core i5), there are still more than 19 ms remaining for a low-cost processor solution.

Future work is oriented to implement the measurement procedure in autonomous equipment within the industrial scenario to deal with new kinds of electrical disturbances that appear in the SG as a consequence of the massive introduction of DERs, which also triggers the need for more measurement points along the whole measurement chain.

Acknowledgments: This research was supported by the Spanish Ministry of Economy, Industry and Competitiveness in the work flow of the State Plan of Excellency and Challenges for Research, via the project TEC2016-77632-C3-3-R-Control and Management of Isolable NanoGrids: Smart Instruments for Solar forecasting and Energy Monitoring (COMING-SISEM), which involves the development of new measurement techniques applied to monitor the PQ in micro-grids. Additionally, we express our gratitude to the Andalusian Government for funding the Research Group PAIDI-TIC-168 in Computational Instrumentation and Industrial Electronics (ICEI).

Author Contributions: Juan-José González-de-la-Rosa proposed the spectral kurtosis as a tool to monitor PQ events, and designed the experiment and the paper layout; Agustín Agüera-Pérez designed the software and the experiment strategy with José-Carlos Palomares-Salas; Olivia Florencias-Oliveros selected the signals from the database and arranged the instrumentation; José-María Sierra-Fernández contributed to the optimization of the spectral kurtosis.

Conflicts of Interest: The authors declare no conflict of interest.

References

1. European Committee for Electrotechnical Standardization. *EN 50160: Voltage Characteristics of Electricity Supplied by Public Electricity Networks*; European Committee for Electrotechnical Standardization: Madrid, Spain, 2010.
2. Milanović, J.; Meyer, J.; Ball, R.; Howe, W.; Preece, R.; Bollen, M.H.; Elphick, S.; Čukalevski, N. International Industry Practice on Power-Quality Monitoring. *IEEE Trans. Power Deliv.* **2014**, *29*, 934–941.
3. Rönneberg, S.K.; Bollen, M.H.; Amaris, H.; Chang, G.W.; Kocewiak, I.Y.G.L.H.; Meyer, J.; Olofsson, M.; Ribeiro, P.F.; Desmeti, J. On waveform distortion in the frequency range of 2kHz–150 kHz-Review and research challenges. *Electr. Power Syst. Res.* **2017**, *150*, 1–9.
4. De la Rosa, J.J.G.; Agüera-Pérez, A.; Salas, J.C.P.; Sierra-Fernández, J.M.; Moreno-Muñoz, A. A novel virtual instrument for power quality surveillance based in higher-order statistics and case-based reasoning. *Measurement* **2012**, *45*, 1824–1835.
5. Vrabie, V.; Granjon, P.; Serviere, C. Spectral Kurtosis: From definition to application. In Proceedings of the IEEE-EURASIP International Workshop on Nonlinear Signal and Image Processing (NSIP'2003), Grado, Italy, 8–11 June 2003; Volume 1, pp. 1–5.
6. De-la Rosa, J.J.G.; Sierra-Fernández, J.M.; Palomares-Salas, J.C.; Agüera-Pérez, A.; Jiménez-Montero, A. An Application of Spectral Kurtosis to Separate Hybrid Power Quality Events (Special Issue Smart Metering). *Energies* **2015**, *8*, 9777–9793.
7. Eto, J.; Koomey, J.; Lehman, B.; Martin, N.; Mills, E.; Webber, C.; Worrell, E. *Scoping Study on Trends in the Economic Value of Electricity Reliability to the U.S. Economy*; Technical Report LBNL-47911; Energy Analysis Department Environmental Energy Technologies Division E. O. Lawrence Berkeley National Laboratory: Berkeley, CA, USA, 2001.
8. IEEE Standard 1100. *IEEE Recommended Practice for Powering and Grounding Electronic Equipment*; Technical Report Emerald Book; Institute of Electrical and Electronics Engineers: Piscataway, NJ, USA, 2005.

9. Liu, W.H.E. Classification and correlation of monitored power quality events. In Proceedings of the IEEE Power Engineering Society Summer Meeting, Edmonton, AB, Canada, 18–22 July 1999; Volume 1, pp. 481–286.
10. Daponte, P.; Penta, M.D.; Mercurio, G. TransientMeter: A Distributed Measurement System for Power Quality Monitoring. *IEEE Trans. Power Deliv.* **2004**, *19*, 456–463.
11. Liu, W. Analysis of monitored power quality data. *Proc. IEEE Power Eng. Soc. Summer Meet.* **1999**, *1*, 320–324.
12. Wagner, V.E.; Andreshak, A.A.; Staniak, J.P. Power quality and factory automation. In Proceedings of the IEEE Industry Applications Society Annual Meeting, Pittsburgh, PA, USA, 2–7 October 1988; Volume 2, pp. 1391–1396.
13. Wagner, V.E.; Andreshak, A.A.; Staniak, J.P. Power quality and factory automation. *IEEE Trans. Ind. Appl.* **1990**, *26*, 620–626.
14. Rauch, G.; Sabin, D.; McGranaghan, M.; Sundaram, A. Implementing system-wide power quality monitoring plans. In Proceedings of the IEEE Transmissions and Distribution Conference, Los Angeles, CA, USA, 15–20 September 1996; Volume 1, pp. 37–44.
15. Sawyer, D. Nonstop monitoring [power quality]. *Inst. Electr. Eng. Rev.* **1999**, *45*, 126–127.
16. Qiu, X.; Wimmer, W. Applying object-orientation and component technology to architecture design of power system monitoring. In Proceedings of the International Conference on Power System Technology, Perth, WA, Australia, 4–7 December 2000; Volume 2, pp. 589–594.
17. Shakarjian, D.R.; Standler, R.B. AC power disturbance detector circuit. *IEEE Trans. Power Deliv.* **1991**, *6*, 536–540.
18. Bucci, G.; Fiorucci, E.; Lani, C. Digital measurement station for power quality analysis in distributed environments. In Proceedings of the 18th IEEE Instrumentation and Measurement Technology Conference, Budapest, Hungary, 21–23 May 2001; Volume 1, pp. 368–373.
19. Young, C.P.; Juang, W.L.; Devaney, M.J. Real-Time Intranet-Controlled Virtual Instrument Multiple-Circuit Power Monitoring. *IEEE Trans. Instrum. Meas.* **2000**, *49*, 579–584.
20. Kilter, J.; Meyer, J. Case Studies for Power Quality Monitoring in Public Distribution Grids—Some Results of Working Group CIGRE/CIREC C4.112. In Proceedings of the Electric Power Quality and Supply Reliability Conference (PQ), Rakvere, Estonia, 11–13 June 2014; Volume 2, pp. 85–92.
21. Makinen, A.; Parkki, M.; Jarventausta, P.; Kortessluoma, M.; Verho, P.; Seesvuori, V.; Seesvuori, R.; Rinta-Opas, A. Power quality monitoring as integrated with distribution automation. In Proceedings of the 16th International Conference and Exhibition on Electricity Distribution, 2001. Part 1: Contributions, CIREC, Amsterdam, The Netherlands, 18–21 June 2001; Volume 2, pp. 1–5.
22. Ribeiro, M.V.; Marques, C.A.G.; Duque, C.A.; Cerqueira, A.S.; Pereira, J.L.R. Detection of Disturbances in Voltage Signals for Power Quality Analysis Using HOS. *EURASIP J. Adv. Signal Process.* **2007**, *2007*, 1–13.
23. Bollen, M.H.J.; Gu, I.Y.H.; Axelberg, P.G.V.; Styvaktakis, E. Classification of Underlying Causes of Power Quality Disturbances: Deterministic versus Statistical Methods. *EURASIP J. Adv. Signal Process.* **2007**, *2007*, 1–17.
24. De la Rosa, J.J.G.; Agüera-Pérez, A.; Salas, J.C.P.; Sierra-Fernández, J.M.; Moreno-Muñoz, A. Higher-order statistics: Discussion and interpretation. *Measurement* **2013**, *46*, 2816–2827.
25. IEEE Standard 1159. *IEEE Recommended Practice for Monitoring Electric Power Quality*; Technical Report; Institute of Electrical and Electronics Engineers, 3 Park Avenue: New York, NY, USA, 2009.
26. International Electrotechnical Commission. *IEC 61000-4-7: Testing and Measurement Techniques. General Guide on Harmonics and Interharmonics Measurements and Instrumentation, for Power Supply Systems and Equipment Connected Thereto*; International Electrotechnical Commission: Madrid, Spain, 2002.
27. International Electrotechnical Commission. *IEC 61000-4-30: Testing and Measurement Techniques. Power Quality Measurement Methods*; International Electrotechnical Commission: Madrid, Spain, 2008.
28. IEEE Standard 519. *IEEE Recommended Practice and Requirements for Harmonic Control in Electric Power Systems*; Technical Report; Institute of Electrical and Electronics Engineers, 3 Park Avenue: New York, NY, USA, 2009.

